

oml



3 4456 0283935 6

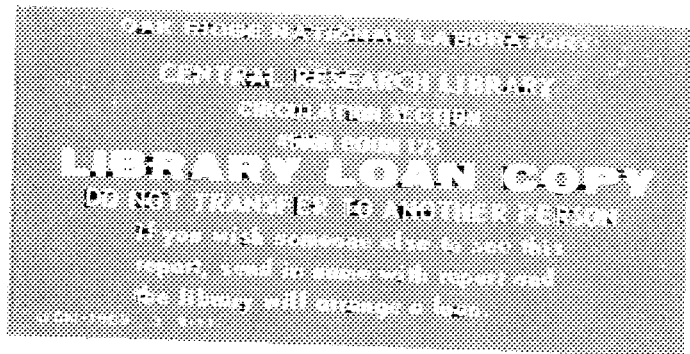
ORNL/TM-10822

OAK RIDGE
NATIONAL
LABORATORY

MARTIN MARIETTA

Ignition and Steady-State Current Drive Capability of INTOR Plasma

N. A. Uckan



OPERATED BY
MARTIN MARIETTA ENERGY SYSTEMS, INC.
FOR THE UNITED STATES
DEPARTMENT OF ENERGY

Printed in the United States of America. Available from
National Technical Information Service
U.S. Department of Commerce
5285 Port Royal Road, Springfield, Virginia 22161
NTIS price codes—Printed Copy: A03; Microfiche A01

This report was prepared as an account of work sponsored by an agency of the United States Government. Neither the United States Government nor any agency thereof, nor any of their employees, makes any warranty, express or implied, or assumes any legal liability or responsibility for the accuracy, completeness, or usefulness of any information, apparatus, product, or process disclosed, or represents that its use would not infringe privately owned rights. Reference herein to any specific commercial product, process, or service by trade name, trademark, manufacturer, or otherwise, does not necessarily constitute or imply its endorsement, recommendation, or favoring by the United States Government or any agency thereof. The views and opinions of authors expressed herein do not necessarily state or reflect those of the United States Government or any agency thereof.

ORNL/TM-10822
Dist. Category UC-420

Fusion Energy Division

**IGNITION AND STEADY-STATE CURRENT DRIVE
CAPABILITY OF INTOR PLASMA**

N. A. Uckan

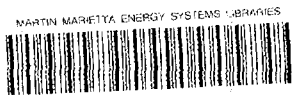
Presented at the 8th Topical Meeting on the Technology of Fusion Energy,
Salt Lake City, Utah, October 9-13, 1988

Date Published: November 1988

Prepared by the
OAK RIDGE NATIONAL LABORATORY
Oak Ridge, Tennessee 37831
operated by
MARTIN MARIETTA ENERGY SYSTEMS, INC.
for the
U.S. DEPARTMENT OF ENERGY
under contract DE-AC05-84OR21400

CONTENTS

ABSTRACT	v
1. INTRODUCTION	1
2. IGNITION CAPABILITY	5
3. STEADY-STATE CURRENT DRIVE CAPABILITY	10
REFERENCES	13



ABSTRACT

The confinement capability of the INTOR plasma for achieving ignition and noninductively driven, $Q > 5$ steady-state operation has been assessed for various energy confinement scaling laws and current drive schemes by using a global power balance model. Plasma operation contours are used to illustrate the boundaries of the operating regimes in density-temperature (n - T) space. Results of the analysis indicate a very restricted capability (if any) for ignition and a limited flexibility in driven modes of operation in the INTOR (8-MA) design. Nearly a factor of two increase in plasma current (through stronger plasma shaping) could improve the feasibility of ignition in INTOR.

1. INTRODUCTION

A global power balance model has been used to evaluate the confinement capability of the INTOR¹ plasma. The feasibility of achieving ignition and noninductively driven, $Q > 5$ steady-state operation has been assessed for various confinement scaling laws and current drive schemes. Parameters used are given in Table I. Physics models and assumptions are summarized in Table II.

The confinement assumptions (Table II) are similar to those developed for the Compact Ignition Tokamak (CIT)² and the International Thermonuclear Experimental Reactor (ITER) studies.³ For noninductive current drive (CD), results from Fisch,⁴ Ehst,⁵ and the INTOR workshop⁶ are used. Details of the global model are given in Ref. 7. The various terms in the power balance are evaluated assuming representative density (a square-root parabolic, $\alpha_n = 0.5$) and temperature (a parabolic, $\alpha_T = 1$) profiles. The fuel mixture is taken as 50-50 deuterium-tritium (D-T) plasma with an effective charge $Z_{\text{eff}} = 1.5$ [$\Delta Z_{\text{eff}} = 0.1$ due to thermal alphas ($n_\alpha/n_e \approx 5\%$) and $\Delta Z_{\text{eff}} = 0.4$ due to carbon and oxygen impurities (with $n_C/n_O \approx 3$)]. In addition to the usual conduction and convection losses, only the bremsstrahlung radiation is considered; line radiation and synchrotron radiation are neglected. Plasma operation contours are used to illustrate the boundaries of the operating regimes in density-temperature (n - T) space. The physics requirements and prime operating scenario for (inductively driven) ignited plasmas differ from those of the noninductively driven plasmas, as illustrated in Fig. 1. Figure 1 shows a typical plasma parameter operating space indicating ignition and specified $Q = Q_0$ contours, along with density and beta limits and a constraint imposed by a given current drive scheme. Subject to the limits (if applicable) and constraints imposed, the shaded regions in the figure correspond to operating windows either for ignition or for $Q \geq Q_0$. For the INTOR (8-MA) plasma, results of our analysis presented in the following sections indicate a very restricted capability for ignition and a limited flexibility in driven modes of operation.

Table I.
INTOR Machine and Plasma Parameters

Design Parameters ³	
Major radius, R (m)	5.0
Minor radius, a (m)	1.2
Elongation, $\kappa = b/a$ (at 95% flux)	1.6
Triangularity, δ (at 95% flux)	0.25
Toroidal field on axis, B (T)	5.5
Plasma current, I (MA)	8.0
Calculated Parameters	
Aspect ratio, $A = R/a$	4.2
Plasma volume (m ³)	227
Plasma surface area (m ²)	328
Wall (chamber) area (m ²)	352
Cylindrical q , q_* (at 95%)	1.9
MHD q , q_ψ (at 95%)	2.2
Troyon beta limit (%)	
$\beta_{\text{crit}} = 3I/aB$	3.64
$(\beta_{\text{crit}} = 4I/aB)$	4.85) ^a
Density limit (10 ²⁰ m ⁻³)	
Murakami-Hugill, $\langle n_{\text{mu}} \rangle = 1.5B/Rq_*$	0.87
Greenwald, $\langle n_{\text{gr}} \rangle \approx 0.65I/\pi a^2$	1.15
$\langle n(\text{at } \beta_{\text{total}} = \beta_{\text{crit}}, T = 10 \text{ keV}) \rangle$	1.28
(Murakami-like, $\langle n_{\text{max}} \rangle \approx 1.5B/R$)	1.65) ^a

^a INTOR assumption (see Ref. 3).

Table II.
Physics Models and Assumptions¹⁻¹⁴

<u>Confinement:</u>	$(1/\tau_E)^2 = (1/\tau_{EOH})^2 + (1/\tau_{Eaux})^2$ or $\tau_E = \min[\tau_{Eaux}; \tau_{EOH}]$ with $\tau_{EOH} = \tau_{NA}$ and $\tau_{Eaux} = f \times \tau_E(\text{L-mode})$ [or $\tau_{Eaux} = \tau_E(\text{H-mode})$]
Neo-Alcator	$\tau_{NA} = 0.07 n_{20} a R^2 q_*$
Kaye-Goldston ⁸	$\tau_{KG} = 0.055 I^{1.24} P^{-0.58} R^{1.65} a^{-0.49} \kappa^{0.28} n_{20}^{0.26} B^{-0.09} (A_i/1.5)^{0.5}$
ASDEX-H ⁹	$\tau_{AXH} = 0.1 I R$
Goldston ¹⁰	$\tau_G = 0.037 I P^{-0.5} R^{1.75} a^{-0.37} \kappa^{0.5} (A_i/1.5)^{0.5}$
T-10 ¹¹	$\tau_{T-10} \approx 0.095 a R B \kappa^{0.5} P^{-(0.4-0.45)} [Z_{eff}^2 I^4 / (a R q_*^3 \kappa^{1.5})]^{(0.08-0.09)}$
Rebut-Lallia ¹²	$\tau_{RL} = C_R I l^{1.5} + C_L n_{20}^{0.75} I^{0.5} B^{0.5} l^{2.75} / P$ $l = (R a^2 \kappa)^{1/3}$, $C_R = 0.024 (A_i/2 Z_{eff})^{0.5}$, $C_L = 0.29 Z_{eff}^{0.25} (A_i/2)^{0.5}$
JAERI ¹³	$\tau_J = C_{J1} \kappa a^2 + C_{J2} I n_{20}^{0.6} B^{0.2} R^{1.6} a^{0.4} \kappa^{0.2} / P$ $C_{J1} = 0.085 A_i^{0.5}$, $C_{J2} = 0.069 G_J(q_*, Z_{eff}) A_i^{0.5}$
Kaye-All ¹⁴	$\tau_{KA} = 0.067 I^{0.85} P^{-0.5} R^{0.85} a^{0.3} \kappa^{0.25} n_{20}^{0.1} B^{0.3} A_i^{0.5}$
Kaye-Big ¹⁴	$\tau_{KB} = 0.105 I^{0.85} P^{-0.5} R^{0.5} a^{0.8} \kappa^{0.25} n_{20}^{0.1} B^{0.3} A_i^{0.5}$
<u>Current drive:</u> ⁴⁻⁶	$\gamma_{CD} = n_{20} I_{CD} R / P_{CD} \approx (T_{10}/60) [J/P]_0$ with $[J/P]_0 \approx \text{constant} \approx 10-40$; or $T_{10} [J/P]_0 \approx \text{const} \approx 10-40$
<u>Units/symbols:</u> ^{2,3,7}	mks, MA, MW, keV, with κ , δ at 95% flux and
n_{20} (10 ²⁰ m ⁻³)	= $\langle n_e \rangle / 10^{20} \text{ m}^{-3}$ = volume-averaged electron density in 10 ²⁰ m ⁻³
T_{10} (10 keV)	= $\langle T \rangle / 10 \text{ keV}$ = density-weighted average temperature in 10 keV ($T_e \approx T_i \approx T$)
q_*	= cylindrical equivalent $q \approx (5a^2 B / R I) [1 + \kappa^2 (1 + 2\delta^2 - 1.2\delta^3)] / 2$
q_Ψ (at 95% flux)	= MHD $q \approx q_* f(\epsilon) \approx q_* [(1.77 - 0.65\epsilon) / (1 - \epsilon^2)^2]$; $\epsilon = a/R$
f	= L-mode enhancement factor (typically, L mode $f = 1$; H mode $f \approx 2$)
A_i	= average atomic mass ≈ 2.5 for a 50:50 D-T plasma
$G_J(q_*, Z_{eff})$	= $Z_{eff}^{0.4} [(15 - Z_{eff}) / 20]^{0.6} [3q_*(q_* + 5) / (q_* + 2)(q_* + 7)]^{0.6}$
Z_{eff}	= effective charge ≈ 1.5 (assumed for this study)
P (MW)	= $W / \tau_E = P_{aux} + P_{OH} + P_\alpha - P_{rad}$ = net "heating" power = [external (heating + CD) + ohmic + alpha - radiation] power
$[J/P]_0$	= dimensionless current drive efficiency
I_{CD} (MA)	= driven current (CD = LH, NB, ...) = $I - I_{bs}$
I_{bs} / I	= neoclassical bootstrap current/total plasma current $\propto (\epsilon^{1/2} \beta_p)$
P_{CD} (MW)	= absorbed current drive power (CD = LH, NB, ...)
<u>Profiles:</u> ^{2,3,7}	$n, T \sim (1 - r^2/a^2)^{\alpha_{n,T}}$ with $\alpha_n = 0.5$ and $\alpha_T = 1.0$

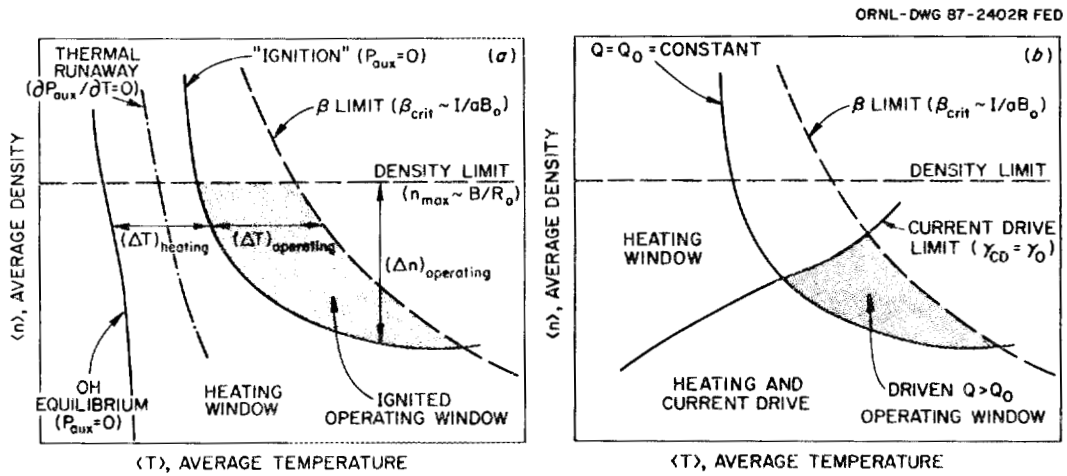


Fig. 1. Typical plasma parameter operating space for (a) an ignited (inductive) and (b) a driven (noninductive) system.

2. IGNITION CAPABILITY

The confinement assessments were made for a variety of scalings,⁸⁻¹⁴ although detailed results are presented only for two empirical scaling expressions that were widely used during the INTOR studies. The first is the combined (in a quadratic mean, see Table II) Kaye-Goldston + neo-Alcator (KG+NA) scaling,⁸ in which all heating (including fusion alpha) power is included in the degradation of confinement. The second is the combined ASDEX-H⁹ + neo-Alcator (AXH+NA) scaling. In both cases the NA component (i.e., ohmic scaling) sets an upper limit on confinement at low plasma densities. Figure 2 shows the ignition contours for both of these scalings. Contours for the KG+NA scaling are for various KG L-mode enhancement factors (ranging from 1.75L to 2L = H). Also plotted are constant beta contours for the Troyon factor $C = \langle \beta (\%) \rangle / (I/aB_0) = 3$ and 4 and the density limits according to the Murakami-Hugill $\langle n_{\text{mu}} \rangle$ and the Greenwald $\langle n_{\text{gr}} \rangle$ scalings (see Table II for corresponding expressions). As a reference, the ignition contour in the limit of NA scaling only is also indicated. Typically, the NA component does not significantly influence the KG scaling (except for very large L-mode enhancement factors). However, the pure ASDEX-H mode scaling is so favorable that it could allow ignition at very low densities, and in such cases the NA limit becomes operative.

As seen from Fig. 2, access for ignition relies on the attainment of some form of an "H-mode." For densities below the Murakami limit ($\langle n_{\text{mu}} \rangle \sim 0.9 \times 10^{20} \text{ m}^{-3}$), ignition appears possible only with the ASDEX-H mode. At higher densities ($>1.2 \times 10^{20} \text{ m}^{-3}$), a small ignition window becomes accessible with the KG H-mode (where $H \geq 2L$). The size of the operating window depends very sensitively on the assumed Troyon beta coefficient and density limit. The INTOR assumption of Troyon factor $C = 4$ (with a low edge safety factor of $q_{\psi} \approx 2.2$) is very optimistic (if not unrealistic) from the MHD stability standpoint, and operation with more realistic CIT-like² ($C \leq 3$) or ITER-like³ ($C \approx 2.5$ to 3) assumptions severely restricts (or eliminates) the ignition window. For the assumed density and temperature profiles, ignition in INTOR with a small margin could be possible only at higher density levels with $C > 3$ and very favorable ASDEX-H-like scalings. Along the beta contour (3.65%), the average neutron wall load is $\sim 0.7 \text{ MW/m}^2$.

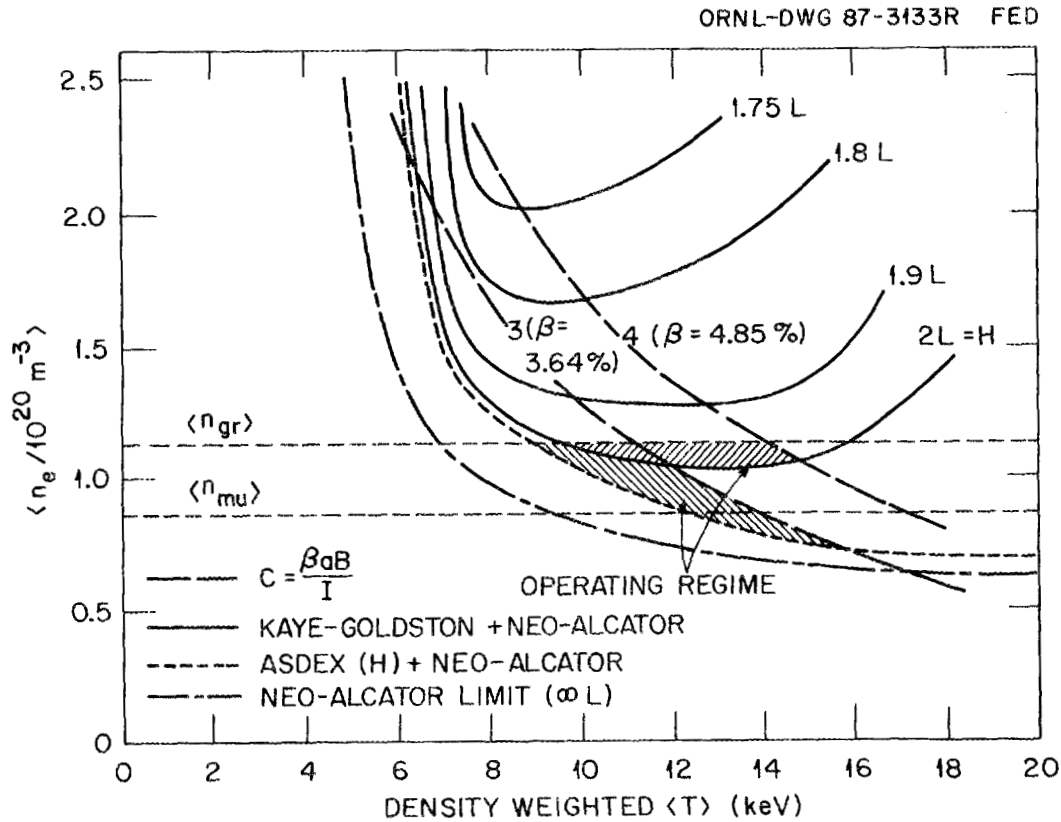


Fig. 2. INTOR ignition contours (solid curves) for various L-mode enhancement factors ($f \sim 1.75$ to 2) of the Kaye-Goldston L-mode scaling, combined (in inverse quadrature) with the neo-Alcator scaling (KG+NA). Also shown are the ignition capability with a combined ASDEX-H + neo-Alcator (short-dash curve) and the limiting neo-Alcator scaling (long-and-short-dash curve). Beta limits corresponding to the Troyon coefficients $C = 3$ and 4 are indicated by long-dash curves. Lines marked by $\langle n_{mu} \rangle$ and $\langle n_{gr} \rangle$ correspond to the Murakami-Hugill and Greenwald density limits. Typical operating windows are indicated by shaded regions.

If the achievable confinement time is below the H-mode enhancement factor of 2, only subignition operation is possible in INTOR. Results for an enhancement factor of 1.5 of the KG L-mode are given in Fig. 3, showing contours of $Q = 5$ and 10 and steady-state auxiliary power required (P_{aux}) to sustain the plasma at a given $\langle n \rangle$ and $\langle T \rangle$. A small $Q = 5$ driven operating window is accessible for $n < n_{\text{mu}}$ and $C \leq 3$ over a temperature range of 8 to 15 keV (see Fig. 3). The required heating power ranges from 20 to 50 MW, producing a fusion power ranging from 100 to 250 MW with an average neutron wall load of 0.3 to 0.7 MW/m². Increase in beta (e.g., Troyon C factor) does not substantially extend the $Q = 5$ operating window for densities $n < n_{\text{mu}}$. For $n \approx n_{\text{gr}}$, $Q \approx 7$ around $T \sim 10$ keV. If no density limit is imposed (except the beta limit), a small $Q \sim 10$ operating window becomes accessible around $n \geq 1.5 \times 10^{20}$ m⁻³ and $T \sim 7$ to 9 keV with $P_{\text{aux}} \sim 30$ MW.

The recent assessment of the experimental data base¹⁴ indicates that both the KG and the AXH scalings are too optimistic. Table III summarizes the INTOR ignition requirements for these and other widely used scaling expressions⁸⁻¹⁴ (see Table II). Given in the table are the minimum L-mode enhancement factors needed for ignition, evaluated at various operational (n , β) limits. In nearly all cases (except for ASDEX H-mode), required enhancement factors over L-mode vary from as low as $f \geq 2$ to as high as $f \gg 3$ (typically, 4 to 6), all of which are well above the enhancement factors observed in the present H-mode experiments (even at low power levels). Nearly a factor of two increase in plasma current (through stronger plasma shaping) could improve the feasibility of ignition in INTOR.

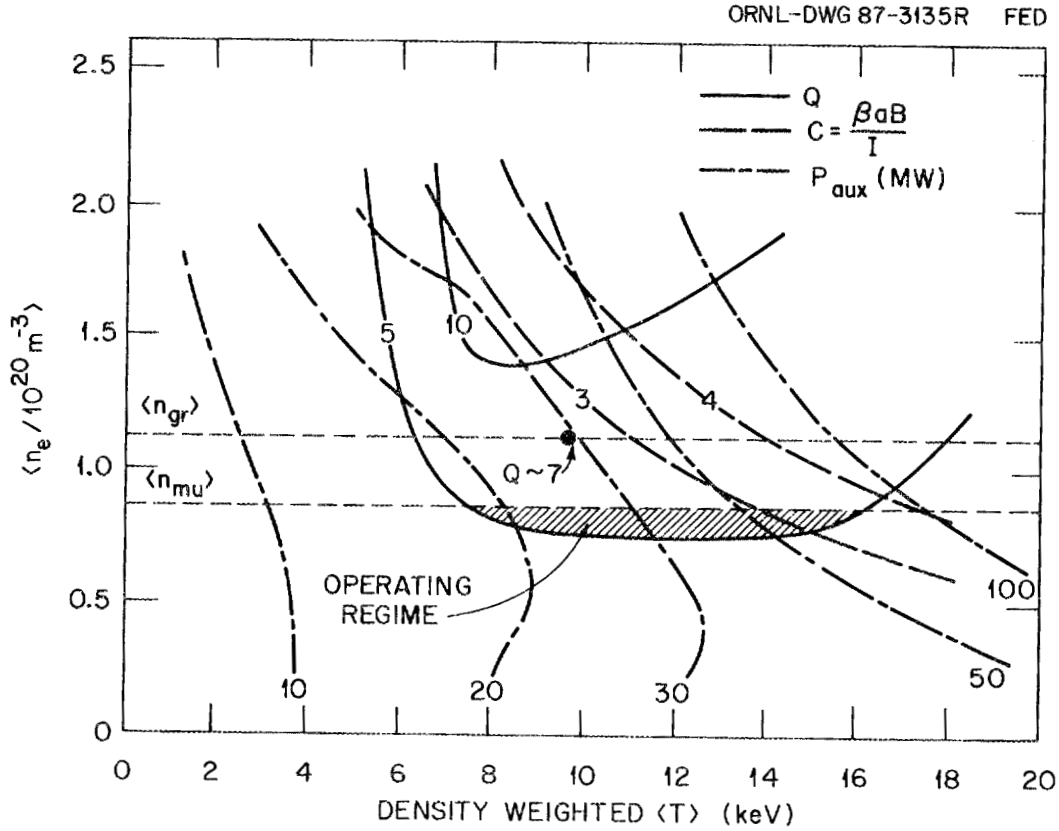


Fig. 3. Steady-state auxiliary power and constant $Q = 5$ and 10 contours for inductively maintained INTOR plasma. Confinement model: Kaye-Goldston + neo-Alcator with an L-mode enhancement factor $f = 1.5$. A typical operating regime bounded by $Q \geq 5$, $n \leq n_{\text{mu}}$, and $\beta \leq \beta_{\text{crit}}$ is indicated by the shaded region.

Table III.
 INTOR Ignition Capability:
 L-mode Enhancement Factor (f) Needed for Ignition
 for Various Confinement Scalings⁸⁻¹⁴
 (Evaluated at Several Operational Limits)

Confinement Scaling	f (evaluated at $T \approx 10$ keV)		
	$n = n_{\text{mu}}$	$n = n_{\text{gr}}$	$\beta = \beta_{\text{crit}}$
Neo-Alcator (NA)	~ Ignited	Ignited	Ignited
ASDEX-H (AXH)			
AXH+NA	Not ignited	Ignited	Ignited
min[AXH; NA]	~ Ignited	Ignited	Ignited
Kaye-Goldston (KG)			
KG+NA	$\gg 3$	≥ 2	≥ 1.9
min[KG; NA]	≥ 2	≥ 1.9	≥ 1.9
Goldston (G)			
G+NA	$\gg 3$	≥ 2.6	≥ 2.5
min[G; NA]	≥ 2.4	> 2.4	> 2.4
T-10 (T-10)			
min[T-10; NA]	≥ 2.2	≥ 2.1	≥ 2.1
Rebut-Lallia (RL)			
min[RL; NA]	≥ 2.3	≥ 2.2	≥ 2.1
JAERI (J)			
min[J; NA]	≥ 3.5	≥ 3.4	≥ 3.4
Kaye-all (KA)			
min[KA; NA]	≥ 3.7	≥ 3.6	≥ 3.6
Kaye-big (KB)			
min[KB; NA]	≥ 3.8	≥ 3.7	≥ 3.7

2. STEADY-STATE CURRENT DRIVE CAPABILITY

To determine the extent of the operating window in a noninductively driven case, it is necessary to introduce some specific schemes for driving the current. Possible options for noninductive current drive include high-energy neutral beams (NB), lower hybrid (LH) slow waves, electron cyclotron (EC) waves, and ion cyclotron (IC) fast waves.³⁻⁶ The neoclassical bootstrap (bs) contribution to the total plasma current could also be substantial ($I_{bs}/I \propto \epsilon^{1/2} \beta_p \sim 30\%$). Some of these current drive techniques (NB, EC, IC) are capable of driving the current in the central portion of the plasma, whereas LH waves drive the current in the outer portion of the plasma. Therefore, a combination of techniques (NB+LH+bs, EC+LH+bs, IC+LH+bs, etc.) may be needed to obtain desired current profiles and current drive efficiencies. In all cases, the current drive figure of merit (global efficiency) is defined as

$$\gamma_{CD} = n_{20} I_{CD} R / P_{CD} = (T_{10}/60) [J/P]_0,$$

where (see Table II) $n_{20} = \langle n_e \rangle / 10^{20} \text{ m}^{-3}$ is the volume-averaged electron density, $T_{10} = \langle T \rangle / 10 \text{ keV}$ is the density-weighted average temperature, I_{CD} is the driven current (MA), P_{CD} is the (absorbed) current drive power (MW), and $[J/P]_0$ is the dimensionless current drive efficiency. In general, $[J/P]_0$ is not constant; it depends on temperature and other physical quantities (such as beam energy and aiming, LH refractive index and accessibility, T_e , Z_{eff} , etc.). Typically,⁴⁻⁶ CD efficiencies (for a range of parameters representative of NB, LH, EC, IC, etc.) are $[J/P]_0 \approx \text{const} \sim 10-40$ or $T_{10} [J/P]_0 \approx \text{const} \sim 10-40$, which yields

$$\gamma_{CD} \sim (0.2-0.6) (T_{10})^x \quad \text{with } x \sim 0-1.$$

Here the range represents “nominal” and “optimistic” levels of the current drive efficiency, which will be used to determine the envelope of the noninductively driven operating regimes in INTOR.

Results of our analyses for a range of current drive schemes with various efficiencies indicate that a full, 8-MA noninductive current drive capability with a reasonable wall loading is not likely to exist in INTOR. However, it may be possible to assist the ohmic-

inductive capability by using, for example, an LH wave or an NB to drive some fraction of the plasma current (I_{CD}/I). For example, with an L-mode enhancement factor of 2 (KG+NA scaling), a $Q \geq 5$ window with 0.3 to 0.7 MW/m² of wall loading appears to be accessible for 25–50% fractional current drive by LH or NB. A possible bootstrap contribution (up to 30%) may improve these fractional limits.

A specific example for KG+NA scaling with an L-mode enhancement factor of 1.5 is given in Fig. 4, which shows a $Q = 5$ contour and the boundaries of current drive for various schemes with efficiencies γ_{CD} ranging from nominal levels, $\gamma_{CD} = 0.3$ or $0.3T_{10}$, to very optimistic levels with substantial bootstrap contribution, $\gamma_{CD} = 0.8$ or $0.8T_{10}$. With nominal current drive efficiencies, only $Q < 5$ operation is possible when $\langle T \rangle$ is above 16 to 20 keV, $\langle n \rangle$ is around 0.5 to $0.8 \times 10^{20} \text{ m}^{-3}$, and beta is near that with C around 3 to 4, requiring a current drive power of 50 to 100 MW. Steady-state operation with $Q \geq 5$ is accessible only if the optimistic levels of current drive efficiencies with substantial bootstrap contribution are assumed. In this case, current drive power levels remain below 50 MW with a small operating window (shaded region in Fig. 4) around $\langle T \rangle \sim 12\text{--}15 \text{ keV}$, $\langle n \rangle \sim 0.8\text{--}1 \times 10^{20} \text{ m}^{-3}$.

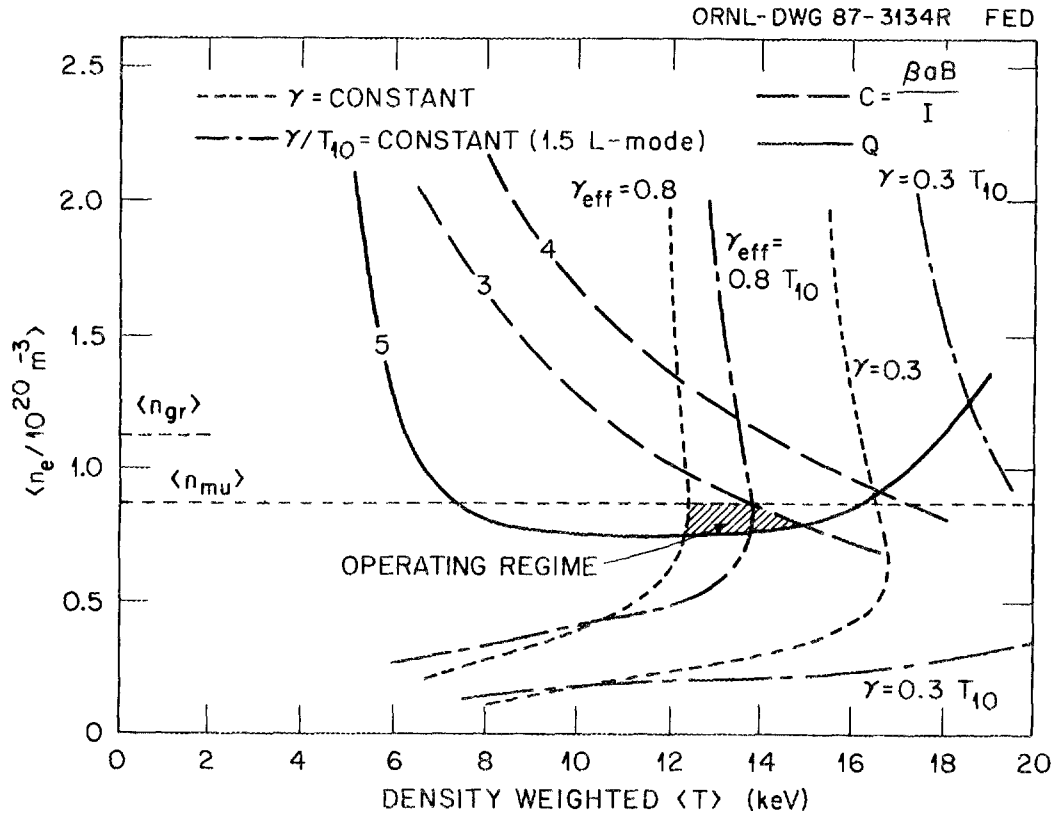


Fig. 4. Boundaries of INTOR steady-state operating space with noninductive current drive. Confinement model: Kaye-Goldston + neo-Alcator with an L-mode enhancement factor $f = 1.5$. Curves representing current drive boundaries are for nominal levels with $\gamma = 0.3$ and $0.3T_{10}$ and optimistic levels with $\gamma_{\text{eff}} = 0.8$ and $0.8T_{10}$, which include substantial bootstrap current. These current drive boundaries are the locus of points where the current drive power required to drive a specified current (8 MA) equals the auxiliary power needed to satisfy the power balance. Accessible operating regimes (in n - T space) are those on and below the current drive boundaries represented by γ or γ/T contours.

REFERENCES

1. "International Tokamak Reactor Phase Two A, Part II," International Atomic Energy Agency, Vienna (1986); "International Tokamak Reactor Phase Two A, Part III," International Atomic Energy Agency, Vienna (to be published).
2. R. PARKER et al., "CIT Physics Design Description," AE-880112-PPL-01, Princeton Plasma Physics Laboratory (1988); D. POST et al., "Physics Aspects of the Compact Ignition Tokamak," *Phys. Scr.*, **T16**, 89 (1987); J. SHEFFIELD et al., "Physics Guidelines for the Compact Ignition Tokamak," *Fusion Technol.*, **10**, 481 (1986).
3. "ITER Definition Phase Report," International Atomic Energy Agency, Vienna (to be published); ITER Physics Team (presented by D. POST), "ITER: Physics Basis," paper IAEA-CN-50/F-II-1, to appear in *Proc. 12th Int. Conf. Plasma Physics and Controlled Nuclear Fusion Research*, Nice, France, October 12-19, 1988.
4. N. J. FISCH, "Theory of Current Drive in Plasmas," *Rev. Mod. Phys.*, **59**, 175 (1987).
5. D. A. EHST and K. EVANS, Jr., "Multiple Wave Frequency Current Driven Tokamak Reactors in the First Stability Regime," *Nucl. Fusion*, **27**, 1267 (1987).
6. "Fusion Reactor Critical Issues," IAEA-TECDOC-441, International Atomic Energy Agency (1987).
7. N. A. UCKAN, "Relative Merits of Size, Field, and Current on Ignited Tokamak Performance," *Fusion Technol.*, **14**, 299 (1988); N. A. UCKAN and J. SHEFFIELD, "A Simple Procedure for Establishing Ignition Conditions in Tokamaks," *Tokamak Startup*, p. 45, H. Knoepfel, Ed., Plenum Press, New York (1986).
8. S. M. KAYE and R. J. GOLDSTON, "Global Energy Confinement Scaling of Neutral Beam Heated Tokamaks," *Nucl. Fusion*, **25**, 65 (1985).
9. O. GRUBER, "Confinement Regimes in Ohmically and Auxiliary Heated Tokamaks," *Proc. Int. Conf. Plasma Physics*, Lausanne, Switzerland, June 27-July 3, 1984, Vol. 1, p. 67, Commission of the European Communities (1984).
10. R. J. GOLDSTON, "Energy Confinement Scaling in Tokamaks," *Plasma Phys. Controlled Fusion*, **26**, 87 (1984).
11. T-10 GROUP (presented by Yu. V. ESIPCHUK), "Investigation of Energy Confinement in ECH Experiments on T-10," and Yu. V. ESIPCHUK, "Utilization of ECRH Results from T-10 for Reactor Parameter Prognosis," *ITER Specialists' Meeting on Energy Confinement*, May 24-27, 1988, Garching, Federal Republic of Germany (to be published).

12. P.H. REBUT et al. (presented by P.P. LALLIA), "Critical Electron Temperature Gradient Model," *ITER Specialists' Meeting on Energy Confinement*, May 24–27, 1988, Garching, Federal Republic of Germany (to be published); P. P. LALLIA, P. H. REBUT, and M. L. WATKINS, "Chaotic Magnetic Topology and Heat Transport in Tokamaks," JET Report, JET-P(88)05 (January 1988, corrigendum March 1988).
13. K. ODAJIMA and Y. SHIMOMURA, "Energy Confinement Scaling Based on Offset Linear Characteristic," JAERI-M 88-068, Japan Atomic Energy Research Institute (March 1988); Y. SHIMOMURA and K. ODAJIMA, "Empirical Scaling of Incremental Energy Confinement Time of L-Mode Plasma and Comments on Improved Confinement in Tokamaks," *Comments Plasma Phys. Controlled Fusion*, **10**, 207 (1987).
14. S. M. KAYE, "Survey of Energy Confinement Scaling Expressions," *ITER Specialists' Meeting on Energy Confinement*, May 24–27, 1988, Garching, Federal Republic of Germany (to be published).

INTERNAL DISTRIBUTION

1. S. E. Attenberger
2. L. A. Berry
3. R. A. Dory
4. J. L. Dunlap
5. J. D. Galambos
6. J. T. Hogan
7. W. A. Houlberg
8. Y-K. M. Peng
9. R. L. Reid
10. M. J. Saltmarsh
11. T. E. Shannon
12. J. Sheffield
- 13-17. N. A. Uckan
- 18-19. Laboratory Records Department
20. Laboratory Records, ORNL-RC
21. Document Reference Section
22. Central Research Library
23. Fusion Energy Division Library
- 24-25. Fusion Energy Division Publications Office
26. ORNL Patent Office

EXTERNAL DISTRIBUTION

27. M. A. Abdou, School of Engineering and Applied Science, 6288 Boelter Hall, University of California Los Angeles, Los Angeles, CA 90024
28. C. C. Baker, Argonne National Laboratory, Fusion Power Program, Bldg. 205, 9700 South Cass Avenue, Argonne, IL 60439
29. G. Bateman, Plasma Physics Laboratory, Princeton University, P.O. Box 451, Princeton, NJ 08543
30. C. Bolton, Office of Fusion Energy, Office of Energy Research, Germantown ER-55, U.S. Department of Energy, Washington, DC 20545
31. K. Borrass, NET Team, Max-Planck-Institut, Boltzmannstrasse 2, D-8046 Garching bei Muenchen, Federal Republic of Germany
32. J. D. Callen, Department of Nuclear Engineering, University of Wisconsin, Engineering Research Building, 1500 Johnson Drive, Madison, WI 53706
33. D. R. Cohn, 167 Albany St., NW 16-140, Massachusetts Institute of Technology, Cambridge, MA 02139
34. R. W. Conn, Fusion Engineering and Physics Program, 6291 Boelter Hall, University of California Los Angeles, Los Angeles, CA 90024

35. B. Coppi, 77 Massachusetts Avenue, 26-217, Massachusetts Institute of Technology, Cambridge, MA 02139
36. D. H. Crandall, Office of Fusion Energy, Office of Energy Research, Germantown ER-542, U.S. Department of Energy, Washington, DC 20545
37. R. C. Davidson, 77 Massachusetts Avenue, Massachusetts Institute of Technology, Cambridge, MA 02139
38. N. A. Davies, Office of Fusion Energy, Office of Energy Research, Germantown ER-55, U.S. Department of Energy, Washington, DC 20545
39. S. O. Dean, Fusion Power Associates, 2 Professional Drive, Suite 249, Gaithersburg, MD 20760
40. S. R. DeVoto, Lawrence Livermore National Laboratory, P.O. Box 5511, Livermore, CA 94550
41. S. A. Eckstrand, Office of Fusion Energy, Office of Energy Research, Germantown ER-55, U.S. Department of Energy, Washington, DC 20545
42. G. A. Eliseev, I. V. Kurchatov Institute of Atomic Energy, Ploshchad' Akademika Kurchatova 46, Moscow 123182, U.S.S.R.
43. F. Engelmann, NET/ITER Team, Max-Planck-Institut, Boltzmannstrasse 2, D-8046 Garching bei Muenchen, Federal Republic of Germany
44. A. J. Favale, Grumman Aerospace Corporation, MS-A0126, P.O. Box 31, Bethpage, NY 11714
45. H. K. Forsen, Bechtel Group Inc., Research and Engineering, P.O. Box 3965, San Francisco, CA 94119
46. T. K. Fowler, Department of Nuclear Engineering, University of California Berkeley, Etcheverry Hall Room 4153, Berkeley, CA 94720
47. N. Fujisawa, Naka Fusion Research Establishment, Japan Atomic Energy Research Inst., Naka-Machi, Naka-Gun, Ibaraki-ken 311-02, Japan
48. H. P. Furth, Plasma Physics Laboratory, Princeton University, P.O. Box 451, Princeton, NJ 08543
49. J. R. Gilleland, Lawrence Livermore National Laboratory, P.O. Box 5511, Livermore, CA 94550
50. R. J. Goldston, Plasma Physics Laboratory, Princeton University, P.O. Box 451, Princeton, NJ 08543
51. R. W. Gould, Department of Applied Physics, California Institute of Technology, Pasadena CA 91125
52. R. A. Gross, Plasma Resesarch Laboratory, Columbia University, New York, NY 10027
53. C. D. Henning, Lawrence Livermore National Laboratory, P.O. Box 5511, Livermore, CA 94550

54. T. R. James, Office of Fusion Energy, Office of Energy Research, Germantown ER-55, U.S. Department of Energy, Washington, DC 20545
55. R. A. Krakowski, CTR-12, Mail Stop 641, Los Alamos National Laboratory, P.O. Box 1663, Los Alamos, NM 87545
56. G. L. Kulcinski, Department of Nuclear Engineering, University of Wisconsin, Engineering Research Building, 1500 Johnson Drive, Madison, WI 53706
57. B. G. Logan, Lawrence Livermore National Laboratory, P.O. Box 5511, Livermore, CA 94550
58. D. M. Meade, Plasma Physics Laboratory, Princeton University, P.O. Box 451, Princeton, NJ 08543
59. G. H. Miley, Fusion Studies Laboratory, University of Illinois, 214 Nuclear Engineering Laboratory, 103 S. Goodwin Ave., Urbana, IL 61801
60. V. Mukhovatov, I. V. Kurchatov Institute of Atomic Energy, 46 Ulitsa Kurchatova, P.O. Box 3402, Moscow 123182, U.S.S.R.
61. W. M. Nevins, Lawrence Livermore National Laboratory, P.O. Box 5511, Livermore, CA 94550
62. A. Opdenaker, Office of Fusion Energy, Office of Energy Research, Germantown ER-532, U.S. Department of Energy, Washington, DC 20545
63. R. R. Parker, Plasma Fusion Center, Massachusetts Institute of Technology, Cambridge, MA 02139
64. D. E. Post, Plasma Physics Laboratory, Princeton University, P.O. Box 451, Princeton, NJ 08543
65. F. Prevot, Association EURATOM-CEA, Departament de Recherches sur la Fusion Controlee, Centre d'Etudes Nucleaires de Cadarache, 13108 Saint Paul Lez Durance Cedex, Cadarache, France
66. S. Putvinski, I. V. Kurchatov Institute of Atomic Energy, 46 Ulitsa Kurchatova, P.O. Box 3402, Moscow 123182, U.S.S.R.
67. P. H. Rebut, JET Joint Undertaking, Abingdon, Oxon, OX14 3EA, England
68. F. L. Ribe, College of Engineering, FL-10, AERL Bldg., University of Washington, Seattle, WA 98195
69. P. H. Rutherford, Plasma Physics Laboratory, Princeton University, P.O. Box 451, Princeton, NJ 08543
70. W. L. Sadowski, Office of Fusion Energy, Office of Energy Research, Germantown ER-541, U.S. Department of Energy, Washington, DC 20545
71. J. A. Schmidt, Plasma Physics Laboratory, Princeton University, P.O. Box 451, Princeton, NJ 08543
72. C. F. Singer, Fusion Studies Laboratory, University of Illinois, 214 Nuclear Engineering Laboratory, 103 S. Goodwin Ave., Urbana, IL 61801

73. W. M. Stacey, Jr., Georgia Institute of Technology, Fusion Research Center, Atlanta, GA 30332
74. R. D. Stambaugh, General Atomics, P.O. Box 85608, San Diego, CA 92138
75. D. Steiner, Rensselaer Polytechnic Institute, Department of Nuclear Engineering, Troy, NY 12181
76. M. Sugihara, Naka Fusion Research Establishment, Japan Atomic Energy Research Institute, Naka-Machi, Naka-Gun, Ibaraki-ken 311-02, Japan
77. V. T. Tolok, Kharkov Physical-Technical Institute, Academical St. 1, 310108 Karkov, U.S.S.R.
78. V. Varma, Physical Research Laboratory, Navrangpura, Ahmedabad, India
79. H. Weitzner, Courant Institute of Mathematical Sciences, New York University, 251 Mercer Street, New York, NY 10012
80. J. W. Willis, Office of Fusion Energy, Office of Energy Research, Germantown ER-55, U.S. Department of Energy, Washington, DC 20545
81. Bibliothek, Max-Planck-Institut für Plasmaphysik, Boltzmannstrasse 2, D-8046 Garching bei Muenchen, Federal Republic of Germany
82. Bibliothek, Institut für Plasmaphysik, KFA Jülich GmbH, Postfach 1913, D-5170 Jülich, Federal Republic of Germany
83. Bibliothek, KfK Karlsruhe GmbH, Postfach 3640, D-7500 Karlsruhe 1, Federal Republic of Germany
84. Bibliotheque, Service du Confinement des Plasmas, CEA, B.P. No. 6, 92 Fontenay-aux-Roses (Seine), France
85. Bibliotheque, Association EURATOM-CEA, Departement de Recherches sur la Fusion Controlee, Centre d'Etudes Nucleaires de Cadarache, F-13108 Saint Paul Lez Durance Cedex, Cadarache, France
86. Documentation S.I.G.N., Departement de la Physique du Plasma et de la Fusion Controlee, Association EURATOM-CEA, Centre d'Etudes Nucleaires, B.P. 85, Centre du Tri, F-38041 Grenoble, France
87. Bibliotheque, Centre de Recherches en Physique des Plasmas, Ecole Polytechnique Federale de Lausanne, 21 Avenue des Bains, CH-1007 Lausanne, Switzerland
88. Library, Culham Laboratory, UKAEA, Abingdon, Oxfordshire, OX14 3DB, England
89. Library, JET Joint Undertaking, Abingdon, Oxfordshire, OX14 3EA, England
90. Library, FOM Instituut voor Plasma-Fysica, Rijnhuizen, Edisonbaan 14, 3439 MN Nieuwegein, Jutphaas, Netherlands
91. Library, Institute of Physics, Academia Sinica, Beijing, Peoples Republic of China
92. Library, International Centre for Theoretical Physics, P.O. Box 586, I-34100 Trieste, Italy

93. Library, Centro Richerche Energia Frascati, C.P. 65, I-00044 Frascati (Roma), Italy
94. Library, Plasma Research Laboratory, Australian National Laboratory, P.O. Box 4, Canberra, ACT 2601, Australia
95. Thermonuclear Library, Japan Atomic Energy Research Institute, Tokai Research Establishment, Tokai, Naka-gun, Ibaraki-ken 311-02, Japan
96. Library, Plasma Physics Laboratory, Kyoto University, Gokasho Uji, Kyoto, Japan
97. Library, Institute for Plasma Physics, Nagoya University, Chikusa-ku, Nagoya 464, Japan
98. Laboratory for Plasma and Fusion Studies, Department of Nuclear Engineering, Seoul National University, Shinrim-dong, Gwanak-ku, Seoul 151, Korea.
99. Office of the Assistant Manager for Energy Research and Development, Department of Energy, Oak Ridge Operations, Oak Ridge, TN 37830
100. M. Roberts, International Programs, Office of Fusion Energy, Office of Energy Research, Germantown ER-52, U.S. Department of Energy, Washington, DC 20545
101. V. A. Glukhikh, Scientific-Research Institute of Electro-Physical Apparatus, 18861 Leningrad, U.S.S.R.
102. I. Shpigel, Institute of General Physics, U.S.S.R. Academy of Sciences, Ulitsa Vavilova 38, Moscow, U.S.S.R.
103. D. D. Ryutov, Institute of Nuclear Physics, Siberian Branch of the Academy of Sciences of the U.S.S.R., Sovetskaya St. 5, 630090 Novosibirsk, U.S.S.R.
104. B. B. Kadomtsev, I. V. Kurchatov Institute of Atomic Energy, 46 Ulitsa Kurchatova, P.O. Box 3402, Moscow 123182, U.S.S.R.
- 105–142. Given Distribution as shown in DOE/OSTI-4500, Energy Research (Distribution Category UC-420, Magnetic Fusion Energy)